

## A quantum transition from localized to extended states in a classically chaotic system

Francesco Benvenuto<sup>1,\*</sup>, Giulio Casati<sup>1,\*</sup>, Italo Guarneri<sup>2,\*\*</sup>, and Dima L. Shepelyansky<sup>3</sup>

<sup>1</sup> Dipartimento di Fisica dell'Università, Via Celoria 16, I-20133 Milano, Italy

<sup>2</sup> Dipartimento di Fisica Teorica e Nucleare, Università di Pavia, I-27100 Pavia, Italy

<sup>3</sup> Institute of Nuclear Physics, SU-630090 Novosibirsk, USSR

Received January 31, 1991

We study the quantum dynamics of a particle in a one dimensional triangular well under a monochromatic perturbation. Though the classical dynamics is described by the Standard Map, the quantum motion is not always localized. At a certain threshold field intensity, a transition takes place, from a regime of power-localized quasi-energy eigenstates to one of extended states.

Fifteen years of investigations on the quantum mechanics of classically chaotic systems have brought into the light an important phenomenon which has important analogies with the Anderson localization of Solid State Physics. A classical system subjected to an external time-periodic perturbation can enter a chaotic regime if the perturbation is strong enough; in that case, it will indefinitely absorb energy from the external field, in a diffusive way. Quite remarkably, this "diffusive excitation" turns out to be suppressed - or at least severely limited - by quantum interference [1]. This phenomenon is known as dynamical localization. It is present, e.g., in the microwave excitation of hydrogen atoms, and the application of the theory of dynamical localization to that problem has led to some predictions that have been recently confirmed by experiments [2-5].

In spite of the localization phenomenon, hydrogen atoms in microwave fields can be ionized via a quasi-classical diffusive excitation above some threshold field intensity. According to [4] this happens when the localized wave packet would be so large as to significantly populate states lying above the one-photon ionization threshold. In other words the delocalization in the H-atom is due to the presence of continuum.

In this paper we present a study of the classical and quantum dynamics of a particle in an infinite triangular

well, subjected to a monochromatic perturbation. The classical dynamics of this model exhibits a stochastic transition and can be approximately described by a Standard Map. The quantum dynamics is then expected to be dominated by the localization phenomenon. According to our results, this is indeed the case for not too strong fields. However, we also provide theoretical and numerical evidence that delocalization - i.e., indefinite quantum excitation - takes place in the model above a critical perturbation strength. This is an interesting result in many respects.

In the first place, the unperturbed problem has no continuous component in its spectrum (unlike the H-atom); therefore, delocalization must be due to a change in the nature of the Floquet operator, from a point spectrum with localized eigenstates to a continuous spectrum with extended states. To the best of our knowledge, this is the first example of such a transition in a periodically perturbed one-dimensional dynamical system.

Second, delocalization comes as a seemingly paradoxical result in a model which is classically described by the Standard Map; as a matter of fact, the quantized Standard Map is the very prototype of quantum localization. The paradox disappears upon realizing that the variables entering the Standard Map are not a conjugate pair for the model. In order to properly quantize the model one must resort to correct conjugate variables, which lead to a different map. We have here a clear illustration that quantizing classical area preserving maps is not a uniquely defined process. A single classical map may correspond to different quantum dynamics, depending on the way it is embedded in a Hamiltonian system.

Finally, the model has a definite physical significance. It was introduced [6] as a description of the dynamics of bubbles in liquid Helium in the presence of a static field. Under suitable conditions it can also describe the dynamics of surface-state electrons near the surface of liquid helium [7, 8], the motion of ultracold neutrons on oscillating smooth surfaces [9], the dynamics of electrons in doped semiconductors [10].

The system we are going to discuss consists of a ball

\* Also at Istituto Nazionale Fisica Nucleare, Sezione di Milano, I-20133 Milano, Italy

\*\* Also at Istituto Nazionale Fisica Nucleare, Sezione di Pavia, I-27100 Pavia, Italy

elastically bouncing on a fixed wall under the action of a constant field plus a monochromatic perturbation. As introduced by Shimshoni and Smilansky in [6] the model is described by the following one-dimensional Hamiltonian:

$$H(X, P; t) = \frac{P^2}{2} + \varepsilon_0 X + \varepsilon X \cos \omega t \quad X \geq 0 \quad (1)$$

where  $\varepsilon_0$  is the constant field strength,  $\varepsilon$  and  $\omega$  are the oscillating field strength and frequency respectively.

This Hamiltonian would be integrable in the absence of the wall, and it is also integrable if the perturbation amplitude is zero; in both cases the explicit solution is trivially obtained. The time-dependent Hamiltonian (1) can be reduced to a more convenient form, by canonically transforming to a moving reference frame in which the wall oscillates according to  $x_0(t) = -\varepsilon \omega^{-2} \cos \omega t$ . The generating function for such a transformation from old canonical variables  $(X, P)$  (*oscillating field representation*) to new ones  $(x, p)$  (*oscillating wall representation*) is:

$$S(X, p, t) = \left( p - \frac{\varepsilon}{\omega} \sin \omega t \right) \times \left( X - \frac{\varepsilon}{\omega^2} \cos \omega t \right). \quad (2)$$

The new Hamiltonian describes a ball bouncing on an oscillating wall under the action of a constant field. The dynamics is conveniently described by the *impact map* which gives the evolution from immediately after a bounce to immediately after the next [11].

$$\begin{cases} \bar{p} = -p + \varepsilon_0 \Delta t + \frac{2\varepsilon}{\omega} \sin(\omega \Delta t + \phi) \\ \bar{\phi} = \omega \Delta t + \phi \end{cases} \quad \text{mod } 2\pi \quad (3)$$

where  $\phi$  is the phase of the field at the time when a bounce occurs, and the time  $\Delta t$  between bounces is given by the smallest strictly positive solution of the equation:

$$p \Delta t - \frac{\varepsilon_0}{2} (\Delta t)^2 + \frac{\varepsilon}{\omega^2} [\cos(\omega \Delta t + \phi) - \cos \phi] = 0 \quad (4)$$

The mapping (3) takes an especially simple form when the amplitude of the motion between subsequent kicks is much larger than the amplitude of wall oscillations:

$$\bar{p} \approx p + \frac{2\varepsilon}{\omega} \sin \phi \quad \bar{\phi} \approx \phi + \frac{2\omega}{\varepsilon_0} \bar{p} \quad \text{mod } 2\pi. \quad (5)$$

A quantitative condition for the validity of this approximation is:

$$E \geq \frac{\varepsilon \varepsilon_0}{\omega^2} \quad (6)$$

where  $E = (3\pi \varepsilon_0 I)^2 / 2$  is the unperturbed energy and  $I$  the action variable. In practice, numerical simulation showed that (6) is a cautious estimate.

The map (5) is just the Standard Map. Using well-known results [12] it is possible to predict the onset of diffusive excitation in the system, when the chaos parameter  $K = 4\varepsilon \varepsilon_0^{-1}$  becomes larger than one, i.e., when the perturbation amplitude exceeds the critical value  $\varepsilon_{cr}^{(C)} = \varepsilon_0 / 4$ .

The fact that the Standard Map provides a good description of the classical model does not command any similarity of the quantum model with the quantum Kicked Rotator (which is a quantization of the classical Standard Map). As a matter of fact, the variables  $p$  and  $\phi$  in (5) are not a conjugate pair in the full Hamiltonian formulation of the model. The correct conjugate variable to the field phase  $\phi$  is the quantity  $N = E/\omega$ , where  $E$  is unperturbed energy. In the conjugate variables  $(N, \phi)$  the impact mapping (5), on neglecting second order terms in  $\varepsilon$ , takes the form:

$$\begin{aligned} \bar{N} &= N + \frac{2\varepsilon}{\omega^2} \sqrt{2\omega N} \sin(\phi) \\ \bar{\phi} &= \phi + \frac{2\omega}{\varepsilon_0} \sqrt{2\omega N} + O(\varepsilon) \end{aligned} \quad (7)$$

This map is not an area-preserving one. In order to get a canonical map one should insert second order corrections in the first equation and first order corrections in the second one. The latter, however, decrease with increasing  $N$  and for this reason even the approximate form (7) was found to satisfactorily describe the motion in the chaotic regime where orbits rapidly diffuse to high  $N$  values.

The map (7) is the analogue of the Kepler map which was found very helpful in the hydrogen atom problem [4]. A classical analysis of (7) leads to predict the onset of chaos under the same conditions found for the Standard Map description. Above the chaotic threshold  $\varepsilon_{cr}^{(C)} = \varepsilon_0 / 4$  a diffusive growth of  $N$  is observed, according to the Fokker-Planck equation:

$$\frac{\partial f}{\partial \tau} = \frac{1}{2} \frac{\partial}{\partial N} \left( D_N \frac{\partial f}{\partial N} \right) \quad (8)$$

where  $\tau$  is time measured in the number of iterations of the map, i.e. in the number of bounces. The diffusion coefficient  $D_N$  is given, in the random phase approximation by:

$$D_N = 4\varepsilon^2 \omega^{-3} N + O(\varepsilon^4). \quad (9)$$

From the Fokker-Planck equation the evolution in time of an ensemble of orbits initially concentrated at  $N = N_0$  and homogeneously distributed phases  $\phi$  can be found. In particular, the first and second moments of the distribution increase in time according to a linear and a quadratic law respectively, which were well confirmed by numerical computations.

The classical map (7) differs from the Kicked Rotator mainly in that the "kick strength"  $k = 2\epsilon\omega^{-2}(2\omega N)^{\frac{1}{2}}$  increases with  $N$  as  $N^{\frac{1}{2}}$ . However, for any  $N$  this map can be locally approximated by a Standard Map with a local chaos parameter  $K = 4\epsilon\epsilon_0^{-1}$ . In the quantum case  $N$  and  $\phi$  become conjugate operators. As shown in [4], due to the periodicity of  $\sin\phi$  the fractional part of  $N$  is a constant of the motion and  $N$  changes only by integer numbers. This quantum model is in a sense analogous to a quantum Kicked Rotator with kick strength  $k(N)$  depending on  $N$ . Accordingly, the "local" localization length will be  $l(N) \approx k^2(N)/2$ . It is conceivable that, if the diffusion coefficient is almost constant on the scale  $l(N)$ , then the quantum evolution will be localized; instead, if  $l(N)$  is large enough for the diffusion coefficient to appreciably increase over the scale  $l(N)$ , one can expect an unending escape towards higher values of  $N$ . According to a previously developed analysis of the case of inhomogeneous localization [13], a condition for delocalization is that  $l(N) \approx D_N > N$ , which yields

$$\epsilon > \epsilon_{cr}^{(\omega)} = \frac{1}{2}\omega^{\frac{3}{2}} \quad (10)$$

A similar result can be obtained by a different heuristic approach, which also yields some information about the structure of eigenfunctions. This approach rests on the assumption that the local structure of eigenfunctions be approximately the same as for a Kicked Rotator with the same local kick strength. The eigenfunctions of the Kicked Rotator are exponentially localized with a localization length  $l/2$ . Then a quasi-energy eigenfunction of the present model should decay away from a site  $N_0$  according to:

$$\left| \frac{\psi_{N_0+N}}{\psi_{N_0}} \right| \sim \prod_{J=1}^N \exp\left(\frac{-\alpha}{N_0+J}\right) \approx (1+N_0^{-1}N)^{-\alpha} \quad (11)$$

where  $\alpha = 0.5\omega^3\epsilon^{-2}$ . According to this estimate, one should expect a point spectrum with power-localized eigenfunctions for  $2\alpha > 1$  and a continuous spectrum with non-normalizable eigenfunctions for  $2\alpha < 1$ . The threshold  $\alpha = 0.5$  coincides with the previous one (10) apart from a factor 2. Needless to say, the above heuristic arguments can hardly be expected to yield numerically precise estimates; anyway, both of them predict the same functional dependence.

The above qualitative picture may have a counterpart in the theory of Anderson localization, where it was rigorously proved [14] that for a one-dimensional Anderson model in which the disorder decays (away from a fixed site) according to an inverse square-root law, a transition from a regime of power localized states to one of extended states occurs at some critical coupling strength. Notice that in our case the "disorder" is constant, but the coupling strength increases as  $N^{1/2}$ .

We need to stress at this point that the transition to delocalization takes place when the field strength  $\epsilon$  ex-

ceeds both the classical chaos border and the quantum border (10).

This prediction was numerically confirmed by our computer simulations of the quantum evolution in the original *oscillating field* frame. Apart from obvious modifications, the numerical method was the same used for numerical analysis of the hydrogen atom problem, as described in [4] (see also [6]).

This method takes advantage of the fact that the unperturbed problem ( $\epsilon = 0$ ) has a pure point spectrum and a complete set of eigenfunctions  $u_n$ , which are explicitly known together with the corresponding eigenvalues  $E_n$ :

$$u_n(X) = (2\epsilon_0)^{\frac{1}{3}} \frac{\text{Ai}[(2\epsilon_0)^{\frac{1}{3}}X - z_n]}{\text{Ai}'(-z_n)}$$

$$E_n = -\left(\frac{\epsilon_0^2}{2}\right)^{\frac{1}{3}} z_n$$

$$z_n = f\left(\frac{2}{3}\pi\left(n - \frac{1}{4}\right)\right) \quad (12)$$

where "Ai" is the Airy function, the  $\{z_n\}$  its zeroes and:

$$f(x) = -x^{\frac{2}{3}} \left(1 + \frac{5}{48x^2} - \frac{5}{36x^4} + \frac{77125}{82944x^6} + \dots\right) \quad (13)$$

is the auxiliary Airy function of the first kind.

The coefficients of the expansion of the wave function over the unperturbed base satisfy a set of first order differential equations that can be explicitly written by using the matrix elements of the position operator  $\hat{x}$ , as given in [6, 15].

$$\langle n' | \hat{x} | n \rangle = \begin{cases} \left(\frac{1}{2\epsilon_0}\right)^{\frac{1}{3}} \frac{-2}{(z_{n'} - z_n)^2} & n' \neq n \\ \left(\frac{1}{2\epsilon_0}\right)^{\frac{1}{3}} \frac{2}{3} z_n & n' = n \end{cases} \quad (14)$$

The size of the base in our computations ranged from 384 to 768. Initially, only a single unperturbed state  $n_0$  was excited and the resulting quantum dynamics was compared to the classical evolution of an ensemble of orbits with the same value  $n_0$  of the unperturbed action variable and randomly distributed angle variable.

The existence of both a localized and a delocalized regime is demonstrated in Figs. 1, 2. In both these cases, the classical motion is fully chaotic, and the classical diffusion continues over all the integration time. Nevertheless, in Fig. 1 the quantum packet follows this classical spread just for a small number of periods of the field, then it "freezes". Notice that in this "frozen" configuration the wave packet is still far from significantly populating the available basis set (see Fig. 3). On the contrary in Fig. 2 the wave packet continues to spread until the basis is filled.

An enlargement of the size of the basis allows the wave packet to spread for a longer time, until even the new basis is filled (Fig. 2). Instead, in the localized case of

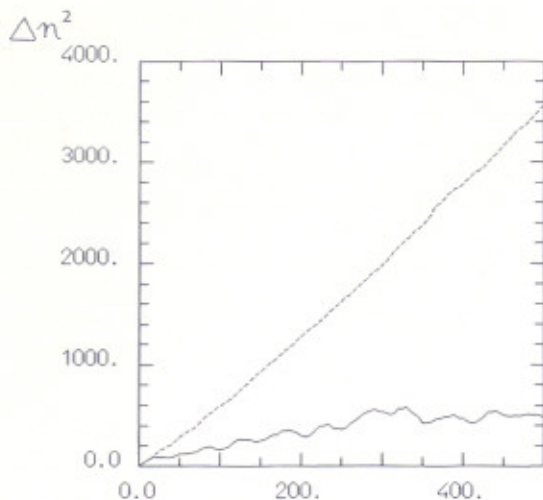


Fig. 1. The numerically computed 2nd moments  $\Delta n^2$  of the distribution in the unperturbed action variable  $n$ , as a function of time (given in number  $t$  of periods of the perturbing field), for  $\omega = 2.52$ ,  $\varepsilon = 0.5$ ,  $\varepsilon_0 = 0.4$ ,  $n_0 = 60$ . The classical motion (dashed line) is diffusive while the quantum (full line) saturates. Here is  $\varepsilon_{cr}^{(Q)} \sim 2.0$

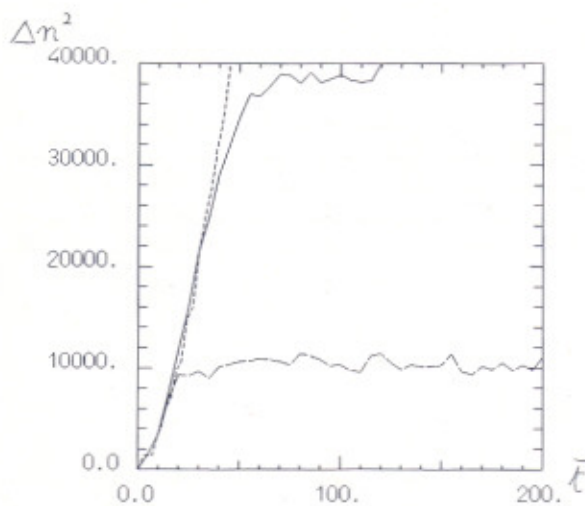


Fig. 2. Same as Fig. 1, with  $\omega = 0.6$ . Here  $\varepsilon_{cr}^{(Q)} \sim 0.2324$ . Two quantum curves are shown with basis size 384 (broken line) and 738 (full line)

Fig. 1, enlarging the basis does not lead to any significant modification of the wave packet evolution.

Due to obvious computational limitations the basis could not be further enlarged. Strictly speaking, the obtained numerical data do not therefore answer the question, whether the observed transition is a real delocalization due to the appearance of a continuous spectral component, or just a localization on a much larger scale. On the other hand, a numerical computation can hardly be expected to yield better evidence than the clear cross-over illustrated by our data.

The above results clearly show that the quantum dynamics of this model is quite different from that of the quantized standard map (5).

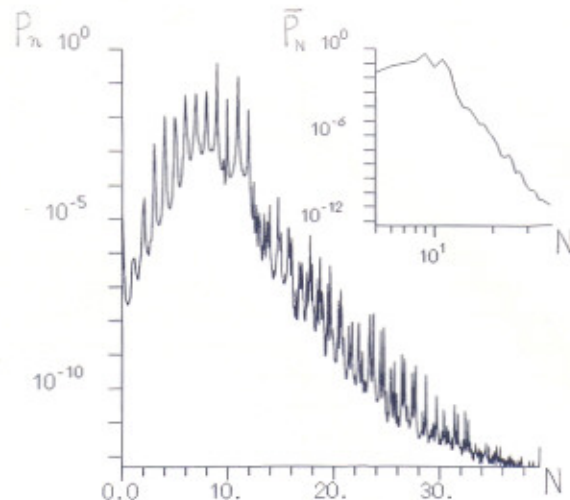


Fig. 3. **a** A localized distribution: the probability of occupation  $P_n$  of the unperturbed state  $n$ , versus  $N$ , in logarithmic scale. Here  $\omega = 2.52$ ,  $\varepsilon = 0.5$ ,  $\varepsilon_0 = 0.4$ ,  $n_0 = 60$ . **b** The total probability  $\bar{P}_N$  within the  $N$ -th photon zone, versus  $N$  in double logarithmic scale

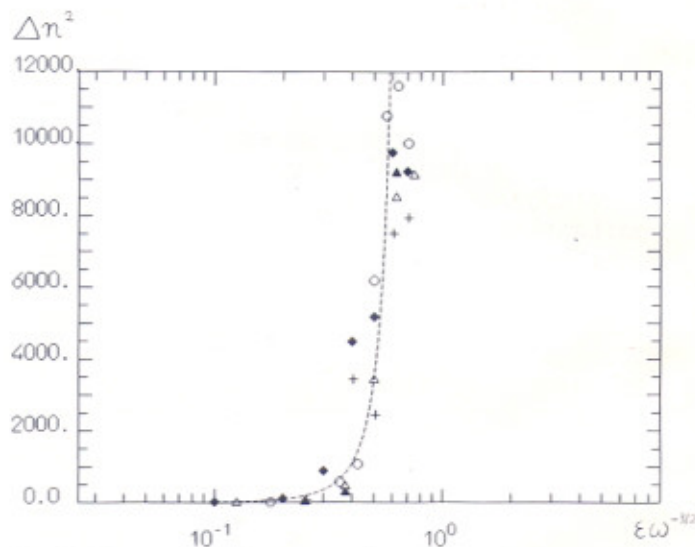


Fig. 4. The spread of the wave packet  $\Delta n^2$  over the unperturbed states (2nd moment of the distribution in  $n$ ), averaged in time from 100 to 200 field periods, versus the decimal logarithm of the variable  $\varepsilon\omega^{-3/2}$  for  $n_0 = 5$ : Full diamonds:  $\omega = 1.00$ ,  $\varepsilon_0 = 0.2$ ; Circles:  $\omega = 2.00$ ,  $\varepsilon_0 = 1.0$ ; Triangles:  $\omega = 2.52$ ,  $\varepsilon_0 = 0.4$ ; Crosses:  $\omega = 4.60$ ,  $\varepsilon_0 = 1.44$  and for  $n_0 = 10$ : Full triangles:  $\omega = 2.52$ ,  $\varepsilon_0 = 0.4$ . The dashed line is drawn to guide the eye

Figure 4 provides a check for the validity of the estimate (10) for the critical field for delocalization. The data in Fig. 4 illustrate how the localization (measured by the spread of the wavepacket after a fixed time) is destroyed upon increasing  $\varepsilon$  while keeping  $\omega$  fixed. The data in Fig. 4 correspond to four different values of  $\omega$ . In each case, the spread increases more or less sharply from 0 to a saturation value (which is determined by the filling up of the finite basis set). In Fig. 4 the spread is plotted (in semi-logarithmic scale) against the variable  $\varepsilon\omega^{-3/2}$  that, according to (10, 11) is the same as  $\varepsilon/\varepsilon_{cr}^{(Q)}$ ,

apart from a numerical factor. The five sets of data in Fig. 4 yield evidence that the localization scales with the variable  $\varepsilon/\varepsilon_{cr}^{(Q)}$  and that  $\varepsilon_{cr}^{(Q)}$  has the predicted functional dependence. Moreover, they suggest that the numerical factor is about 0.5, as in (10).

The steady-state distribution in the localized regime exhibits a remarkable structure. In Fig. 3a we plot one such distribution against the variable  $N = E/\omega$ . The main characteristics of this distribution is a sequence of peaks, equidistant in energy, starting from the initially excited state.

Concerning the overall shape of the distribution, the data provide some clear evidence for a power-like decaying distribution (recall that the quantization of the Standard Map (5) would lead instead to an exponential distribution); see Fig. 3b, which is a bilogarithmic plot of the population of "resonant" zones (i.e. a plot of  $\ln \bar{P}_N$  vs  $\ln N$ , where  $\bar{P}_N$  is the total probability on unperturbed levels  $n$  with energies  $E_n$  lying between  $E_{n_0} + (N - \frac{1}{2})\omega$  and  $E_{n_0} + (N + \frac{1}{2})\omega$ ). With this definition of  $\bar{P}_N$ , Fig. 3b differs from Fig. 3a not only because of a different scaling in the horizontal axis, but also because of a local smoothing.

There is some evidence that the exponent ruling the algebraic decay of the distribution decreases when the delocalization border (10) is approached from below. However, because of the algebraic tail, very large bases must be used for reliably computing this exponent. This is one reason why we could not yet have a full check of the predicted power law (11) for eigenfunctions; our numerical data relate to the decay of the distribution rather

than of the eigenfunctions, and the theoretical relationship between the two types of decay requires further investigations.

This work was performed with the support of Consiglio Nazionale delle Ricerche, Progetto Finalizzato Sistemi Informatici e Calcolo Parallelo.

## References

1. Casati, G., Chirikov, B.V., Izrailev, F.M., Ford, J.: In: Lecture notes in Physics, Vol. 93: Stochastic behavior in classical and quantum Hamiltonian systems. Casati, G., Ford, J. (eds.), p. 334. Berlin, Heidelberg, New York: Springer 1979
2. Galvez, E.J., Sauer, B.E., Moorman, L., Koch, P.M., Richards, D.: Phys. Rev. Lett. **61**, 2011 (1988)
3. Bayfield, J., Casati, G., Guarneri, I., Sokol, D.: Phys. Rev. Lett. **63**, 364 (1989)
4. Casati, G., Guarneri, I., Shepelyansky, D.: IEEE J. Quantum Electron. **24**, 1420 (1988)
5. Casati, G., Guarneri, I., Shepelyansky, D.: Physica A, **163**, 205 (1990)
6. Shimshoni, E., Smilansky, U.: Nonlinearity **1**, 435 (1988)
7. Jensen, R.: Phys. Rev. A **30**, 386 (1984)
8. Berman, G.P., Zaslavsky, G.M., Kolovsky, A.R.: Sov. Phys. JETP **61**, 925 (1985)
9. Frank, A.I.: Priroda **NI**, 30 (1981) (in Russian)
10. Sherwin, Mark.: Private communication
11. Lichtenberg, A.J., Leiberman, M.A.: Regular and stochastic motion. Berlin, Heidelberg, New York: Springer 1983
12. Chirikov, B.: Phys. Rep. **52**, 263 (1979)
13. Chirikov, B., Shepelyansky, D.: Radiofizika **29**, 104 (1986)
14. Delyon, F., Simon, B., Souillard, B.: Ann. Inst. Henri Poincaré **42**, 283 (1985)
15. Gordon, R.: J. Chem. Phys. **51**, 14, Appr. A (1969)